

# A $C^0$ finite element investigation for buckling of shear deformable laminated composite plates with random material properties

B.N. Singh<sup>†</sup>, N.G.R. Iyengar<sup>‡</sup> and D. Yadav<sup>‡</sup>

*Department of Aerospace Engineering, Indian Institute of Technology, Kanpur 208016, India*

**Abstract.** Composites exhibit larger dispersion in their material properties compared to conventional materials due to larger number of parameters associated with their manufacturing processes. A  $C^0$  finite element method has been used for arriving at an eigenvalue problem using higher order shear deformation theory for initial buckling of laminated composite plates. The material properties have been modeled as basic random variables. A mean-centered first order perturbation technique has been used to find the probabilistic characteristics of the buckling loads with different edge conditions. Results have been compared with Monte Carlo simulation, and those available in literature.

**Key words:** finite element method; random variables; buckling; probabilistic characteristics; composite plates.

## 1. Introduction

Laminated composite panels/plates are being widely used in a great variety of engineering applications in aeronautical, mechanical, chemical and other industries over the past two decades. The main reasons for this trend are the outstanding mechanical properties of composites, such as high strength to weight ratio, excellent corrosion resistance and very good fatigue characteristics. Its ability to allow the structural properties to be tailored according to requirements adds to versatility of composites for sensitive applications.

Classical (Kirchhoff) plate theory has been widely used to model plate behaviour, but is adequate only for thin laminates. Since the ratio of the in plane elastic modulus to the transverse modulus is large for composites plates. Kirchhoff theory, which neglects transverse shear deformation, is usually inadequate for the analysis of thick or moderately thick composite plates. Many plate theories have been proposed to include the effect of shear deformation, of which the laminated version of the first order shear deformation theory (FSDT) developed by Reissner (1945) and Mindlin (1951) is the simplest. This theory assumes a linear distribution of the in -plane normal and shear stresses over the thickness, which results in nonzero transverse shear stresses. Higher-order shear deformation theories (HSDT) can overcome the limitations of the FSDT by introducing additional degrees of freedom (DOF). The HSDT proposed by Reddy (1984) not only accounts for transverse shear effects but also produces a parabolic variation of the transverse shear stress through

---

<sup>†</sup> Research Scholar(on leave from MN Regional Engineering College, Allahabad, India)

<sup>‡</sup> Professor

the thickness of the plate.

Considerable research has been done to characterize the buckling response of structures made of composites. Much of the work on buckling response is based on deterministic analysis (e.g., Ghosh and Dey 1994, Moita *et al.* 1996). Relatively very little work has been reported on the buckling response of structures made of composites with random system parameters. Laminated composite plates have random system parameters, such as material properties as a large number of factors are associated with their manufacturing and fabrication processes. So for accurate modeling of system behaviour, it is logical to model the system parameters as random.

Ibrahim (1987) and Manohar and Ibrahim (1999) reviewed number of topics on structural dynamics with parameter uncertainties. Nakagiri *et al.* (1990) have studied simply supported (SS) graphite/epoxy plates with stochastic finite element method (SFEM) taking fiber orientation, layer thickness and number of layers as random variables, and found that the overall stiffness of fiber reinforced plastic (FRP) laminated plates is found out to be largely dependent on the fiber orientation. Leissa and Martin (1990) have analyzed the free vibration and buckling of rectangular composite plates and have established that variation in fiber spacing or redistribution of fibers tend to increase buckling load by 38 percent and the fundamental frequency by 21 percent. Englested and Reddy (1994) studied metal matrix composites based on probabilistic micro mechanics nonlinear analysis. They have used Monte Carlo simulation (MCS) with different probabilistic distributions to incorporate the uncertainty in basic material properties. Vinckenroy and Wilde (1995) in the first part of their work have established a procedure to obtain the best fit for each material property. Further, they have studied the behaviour of the perforated plate and determined the probability distribution of the response. The input variables have been simulated using MCS and SFEM. Salim *et al.* (1998) used the first order perturbation technique (FOPT) with Rayleigh-Ritz formulation to analyze the bending, buckling and vibration of composite plates using classical laminate theory. The RR method can be used only for regular boundary problems. This limitation can be overcome by using FEM.

Yadav and Verma (1997) have studied the buckling response of thin cylindrical shells with random material properties using classical laminate theory and have employed the FOPT for obtaining the second order statistics of the buckling loads. Lin and Kam (2000) have studied the probabilistic failure analysis of transversely loaded laminated composite plates using the first order second moment method. They have modeled the system parameters as random variables (RVs) since, for composite laminates made with prepreg tapes; they have observed very small spatial variability of system parameters.

Singh *et al.* (2001) have analyzed the buckling analysis of laminated cross-ply cylindrical panels with random material properties for all edges simply supported using classical laminate theory, FSDT and HSDT. They have employed first order perturbation technique to obtain the second order statistics. The exact method for mean analysis has been considered. The proposed exact method can only be used for cross-ply panels with all edges simply supported.

The contribution of this paper is the application of a  $C^0$  finite element in conjunction with first order perturbation technique to outline a procedure for the buckling analysis of laminated composite plates with random material properties. The third order shear deformation theory proposed by Reddy (1984) is used. The material properties are treated as basic random variables (Lin and Kam 2000) in the stochastic finite element analysis for determining the second order statistics of buckling loads in laminated composite plates with various boundary conditions.

## 2. Formulation

### 2.1 Displacement field

The rectangular laminated composite plate analyzed is shown in Fig. 1. In the present work the higher order shear deformation theory (Reddy 1984) has been employed to study buckling response of composite laminated plates of thickness  $h$  and subjected to inplane loads. The displacements along  $x$ ,  $y$  and  $z$  directions for arbitrary composite laminated plates are (Reddy 1984)

$$\begin{aligned}\bar{u} &= u + f_1(z)\phi_x + f_2(z)\frac{\partial w}{\partial x}; \\ \bar{v} &= v + f_1(z)\phi_y + f_2(z)\frac{\partial w}{\partial y}; \quad \bar{w} = w;\end{aligned}\quad (1)$$

where  $(\bar{u}, \bar{v}, \bar{w})$  are displacements along the  $(x, y, z)$  coordinates,  $(u, v, w)$  are the corresponding displacements of a point on the middle surface, and  $\phi_x$  and  $\phi_y$  are the rotations at  $z = 0$  of normal to the mid-surface with respect to the  $x$  and  $y$  axes, respectively. The  $f_1(z)$  and  $f_2(z)$  are represented as,

$$f_1(z) = C_1 z - C_2 z^3 \quad \text{and} \quad f_2(z) = -C_4 z^3. \quad (2)$$

Where  $C_1$ ,  $C_2$  and  $C_4$  are constants. The values of these constants are,

$$C_1 = 1; C_2 = C_4 = \frac{4}{3h^2}. \quad (3)$$

From Eq. (1), it is seen that the expressions for in plane displacement  $\bar{u}$  and  $\bar{v}$  involve the derivatives of out of plane displacement  $\bar{w}$ . As a result of this, second order derivatives would be present in the strain vector, thus necessitating the employment of a  $C^1$  continuity for finite element analysis. The complexity and difficulty involved with making a choice of  $C^1$  continuity are well known. This is circumvented by expressing the displacement field in the following form (Shankara and Iyengar 1996):

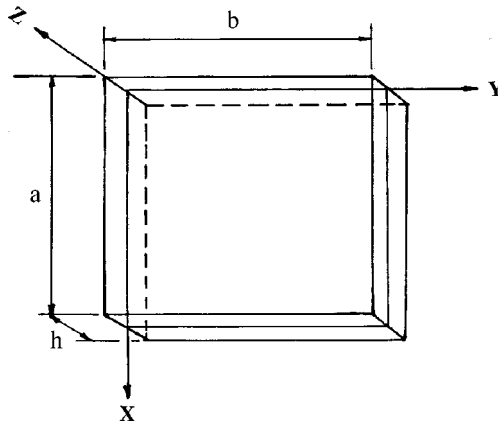


Fig. 1 Geometry of plate element

$$\begin{aligned}\bar{u} &= u + f_1(z)\phi_x + f_2(z)\theta_x; \\ \bar{v} &= v + f_1(z)\phi_y + f_2(z)\theta_y; \quad \bar{w} = w;\end{aligned}\quad (4)$$

where,

$$\theta_x = \frac{\partial w}{\partial x} \text{ and } \theta_y = \frac{\partial w}{\partial y}. \quad (5)$$

It can be seen that the number of degrees of freedom (DOF) per node, by treating  $\theta_x$  and  $\theta_y$  as separate DOFs, increases from 5 to 7 for the HSDT model. However, the strain vector will be having only first order derivatives, and hence a  $C^0$  continuous element would be sufficient for the finite element analysis.

## 2.2 Strain-displacement relations

The strain-displacement relations are obtained by using small deformation theory. The strain vectors corresponding to the displacement field given by Eq. (1) are

$$\begin{aligned}\epsilon_{xx} &= \epsilon_1^0 + z(\kappa_1^0 + z^2 \kappa_1^2); & \epsilon_{yy} &= \epsilon_2^0 + z(\kappa_2^0 + z^2 \kappa_2^2); \\ \epsilon_{yz} &= \epsilon_4^0 + z^2 \kappa_4^1; & \epsilon_{xz} &= \epsilon_5^0 + z^2 \kappa_5^1; & \epsilon_{xy} &= \epsilon_6^0 + z(\kappa_6^0 + z^2 \kappa_6^2),\end{aligned}\quad (6)$$

where

$$\begin{aligned}\epsilon_1^0 &= \frac{\partial u}{\partial x}; \quad \kappa_1^0 = C_1 \frac{\partial \phi_x}{\partial x}; \quad \kappa_1^2 = -C_2 \frac{\partial \phi_x}{\partial x} - C_4 \frac{\partial \theta_x}{\partial x}; \\ \epsilon_2^0 &= \frac{\partial v}{\partial y}; \quad \kappa_2^0 = C_1 \frac{\partial \phi_y}{\partial y}; \quad \epsilon_5^0 = C_1 \phi_x + \frac{\partial w}{\partial x}; \\ \kappa_2^2 &= -C_2 \frac{\partial \phi_y}{\partial y} - C_4 \frac{\partial \theta_y}{\partial y}; \quad \epsilon_4^0 = C_1 \phi_y + \frac{\partial w}{\partial y}; \quad \kappa_4^1 = -3C_2 \phi_y - 3C_4 \theta_y; \\ \kappa_5^1 &= -3C_2 \phi_x - 3C_4 \theta_x; \quad \epsilon_6^0 = \frac{\partial u}{\partial y} + \frac{\partial v}{\partial x}; \quad \kappa_6^0 = C_1 \left( \frac{\partial \phi_y}{\partial x} + \frac{\partial \phi_x}{\partial y} \right); \\ \kappa_6^2 &= -C_2 \left( \frac{\partial \phi_y}{\partial x} + \frac{\partial \phi_x}{\partial y} \right) - C_4 \left( \frac{\partial \theta_y}{\partial x} + \frac{\partial \theta_x}{\partial y} \right).\end{aligned}\quad (7)$$

## 2.3 Strain energy

Using the stress-strain relations, the elastic strain energy of a laminated composite plate can be expressed in terms of strain alone as

$$U = \frac{1}{2} \int_A \{ \bar{\epsilon} \}^T [D] \{ \bar{\epsilon} \} dA; \quad (8)$$

where

$$\{ \bar{\epsilon} \} = [\epsilon_1^0 \ \epsilon_2^0 \ \epsilon_6^0 \ \kappa_1^0 \ \kappa_2^0 \ \kappa_6^0 \ \kappa_1^2 \ \kappa_2^2 \ \kappa_6^2 \ \epsilon_4^0 \ \epsilon_5^0 \ \kappa_4^1 \ \kappa_5^1]^T; \quad (9)$$

$$[D] = \begin{bmatrix} [A1] & [B] & [E] & 0 & 0 \\ [B] & [D1] & [F1] & 0 & 0 \\ [E] & [F1] & [H] & 0 & 0 \\ 0 & 0 & 0 & [A2] & [D2] \\ 0 & 0 & 0 & [D2] & [F2] \end{bmatrix}; \quad (10)$$

with

$$(A1_{ij}, B_{ij}, D1_{ij}, E_{ij}, F1_{ij}, H_{ij}) = \sum_{k=1}^N \int_{z_{k-1}}^{z_k} Q_{ij}^{(k)}(1, z, z^2, z^3, z^4, z^6) dz \text{ for } i, j = 1, 2, 6; \quad (11)$$

$$(A2_{ij}, D2_{ij}, F2_{ij}) = \sum_{k=1}^N \int_{z_{k-1}}^{z_k} Q_{ij}^{(k)}(1, z^2, z^4) dz \text{ for } i, j = 4, 5. \quad (12)$$

where  $\bar{Q}_{ij}^{(k)}$  are the transformed reduced stiffness coefficients of the  $k$ th lamina

## 2.4 External work done

The work done by the in plane forces in producing out of plane displacement ‘ $w$ ’ in domain of small displacements is,

$$\begin{aligned} W &= \frac{1}{2} \int_A \left[ N_x \left( \frac{\partial w}{\partial x} \right)^2 + N_y \left( \frac{\partial w}{\partial y} \right)^2 + 2N_{xy} \left( \frac{\partial w}{\partial x} \right) \left( \frac{\partial w}{\partial y} \right) \right] dA \\ &= \frac{1}{2} \int_A \begin{Bmatrix} w_{,x} \\ w_{,y} \end{Bmatrix}^T \begin{bmatrix} N_x & N_{xy} \\ N_{xy} & N_y \end{bmatrix} \begin{Bmatrix} w_{,x} \\ w_{,y} \end{Bmatrix} dA; \end{aligned} \quad (13)$$

where,  $N_x$ ,  $N_y$  and  $N_{xy}$  are in plane forces.

## 2.5 Finite element model

With advent of computers, finite element method (FEM), has been found to be a very versatile tool for solving complex, real life problem. In the present study, nine noded isoperimetric Lagrangian elements have been employed. The governing equations are developed using variational approach.

### 2.5.1 Prebuckling analysis

The displacement field model given by Eq. (1) may be represented as,

$$\{\hat{u}\} = [N]\{\Lambda\}; \quad (14)$$

where,

$$\{\hat{u}\} = \{u \ v \ w\}^T;$$

$$[N] = \begin{bmatrix} 1 & 0 & 0 & 0 & f_2(z) & 0 & f_1(z) \\ 0 & 1 & 0 & f_2(z) & 0 & f_1(z) & 0 \\ 0 & 0 & 1 & 0 & 0 & 0 & 0 \end{bmatrix};$$

$$\{\Lambda\} = [u \ v \ w \ \theta_y \ \theta_x \ \phi_y \ \phi_x]^T. \quad (15)$$

As mentioned earlier, an isoparametric element is employed for finite element modeling. For this type of element, the displacement vector and the element geometry are represented by the same interpolation functions.

$$\{\Lambda\} = \sum_{i=1}^{NN} \phi_i \{\Lambda\}_i; \quad (16)$$

$$x = \sum_{i=1}^{NN} \phi_i x_i$$

$$y = \sum_{i=1}^{NN} \phi_i y_i \quad (17)$$

where  $\phi_i$  is the interpolation function (Hinton and Owen 1984) for the  $i^{\text{th}}$  node,  $\{\Lambda\}_i$  is the vector of unknown displacements for the  $i^{\text{th}}$  node,  $NN$  is the number of nodes per element and  $x_i$  and  $y_i$  are Cartesian coordinates of the  $i^{\text{th}}$  node.

The strain vectors given in Eqs. (7) and (9) may be written as

$$\{\bar{\epsilon}\} = [L]\{\Lambda\}; \quad (18)$$

where,  $[L]$  is a differential operator (Shankara and Iyengar 1996).

The functional is computed for each element and then summed over all the elements in the domain to get the total functional for the domain. Following this, Eq. (8) can be written as

$$U = \sum_{e=1}^{NE} U^{(e)}$$

$$= \sum_{e=1}^{NE} \frac{1}{2} \int_{A^{(e)}} \{\bar{\epsilon}\}^T [D] \{\bar{\epsilon}\} dA; \quad (19)$$

where,  $NE$  is the number of elements.

From Eqs. (16), (18) and (19), we get

$$U^{(e)} = \{\Lambda\}^{T(e)} [K]^{(e)} \{\Lambda\}. \quad (20)$$

Here  $[K]^{(e)}$  is the element bending stiffness matrix

$$[K]^{(e)} = \frac{1}{2} \int_{A^{(e)}} [BB]^T [D] [BB] dA. \quad (21)$$

Here  $[BB_i]$  is strain displacement matrix for the  $i^{\text{th}}$  node (Shankara and Iyengar 1996).

The element stiffness can be obtained from Eq. (21) by transforming expression in  $x, y$  coordinate system to natural coordinate system  $\xi, \eta$  and adopting numerical integration (Gaussian quadrature).

### 2.5.2 Buckling analysis

Using finite element notation, Eq. (13) may be rewritten as

$$\begin{aligned} W &= \sum_{e=1}^{NE} W^{(e)} \\ &= \sum_{e=1}^{NE} \frac{1}{2} \int_{A^{(e)}} \begin{Bmatrix} w_{,x} \\ w_{,y} \end{Bmatrix}^T \begin{bmatrix} N_x & N_{xy} \\ N_{xy} & N_y \end{bmatrix} \begin{Bmatrix} w_{,x} \\ w_{,y} \end{Bmatrix} dA; \end{aligned} \quad (22)$$

we have,

$$\begin{Bmatrix} w_{,x} \\ w_{,y} \end{Bmatrix} = [L_g] \{ \Lambda \}; \quad (23)$$

where,

$$[L_g] = \begin{bmatrix} 0 & 0 & \frac{\partial}{\partial x} & 0 & 0 & 0 \\ 0 & 0 & \frac{\partial}{\partial y} & 0 & 0 & 0 \end{bmatrix}; \quad (24)$$

Hence Eq. (23) may be rewritten as

$$\begin{aligned} \begin{Bmatrix} w_{,x} \\ w_{,y} \end{Bmatrix} &= [L_g] \sum_{i=1}^{NN} \phi_i \{ \Lambda_i \} \\ &= [BB_g] \{ \Lambda \}^{(e)} \end{aligned} \quad (25)$$

Here  $\{ \Lambda \}^{(e)}$  is the elemental displacement vector and

$$[BB_g] = [[BB_{g1}][BB_{g2}] \dots [BB_{gNN}]] \quad (26)$$

with

$$[BB_{gi}] = [L_g] \phi_i. \quad (27)$$

Adopting similar steps as given in sub section 2.5.1 for prebuckling analysis, Eq. (22) may be written as

$$W^{(e)} = \{ \Lambda \}^{T(e)} \lambda^* [K_g]^{(e)} \{ \Lambda \}^{(e)}. \quad (28)$$

Here,

$$N_x = \lambda^* \bar{N}'_x; \quad N_y = \lambda^* \bar{N}'_y; \quad N_{xy} = \lambda^* \bar{N}'_{xy};$$

and  $\lambda^*$  denotes the buckling load parameter which is a function of the deterministic applied loads as shown above and the  $[K_g]^{(e)}$  is the elemental geometric stiffness matrix given by,

$$[K_g]^{(e)} = \frac{1}{2} \int_{A^{(e)}} [BB_g]^T \begin{bmatrix} \bar{N}'_x & \bar{N}'_{xy} \\ \bar{N}'_{xy} & \bar{N}'_y \end{bmatrix} [BB_g] dA. \quad (29)$$

Adopting numerical integration, the element geometric stiffness can be obtained.

## 2.6 Governing equations

The governing equations for buckling analysis can be derived by using the principle of Total Potential Energy (TPE). This gives

$$\delta(U + V) = 0. \quad (30)$$

where potential energy  $V = -W$ .

Substituting Eqs. (20) and (28) in Eq. (30), ones obtain as:

$$\delta(\{q^*\}^T [K] \{q^*\} - \{q^*\}^T \lambda^* [K_g] \{q^*\}) = 0; \quad (31)$$

where,

$$\{q^*\} = \sum_{e=1}^{NE} \{\Lambda\}^{(e)} - \text{Global displacement vector}$$

$$[K] = \sum_{e=1}^{NE} [K]^{(e)} - \text{Global bending stiffness matrix}$$

$$[K_g] = \sum_{e=1}^{NE} [K_g]^{(e)} - \text{Global geometric stiffness matrix}$$

Eq. (31) can be represented as

$$[[K] - \lambda^* [K_g]] \{q^*\} = 0. \quad (32)$$

The stiffness matrix  $[K]$  is decomposed as

$$[K] = [V]^T [V]; \quad (33)$$

With  $[V]$  being a nonsingular matrix.

Eq. (32) can be written as a standard eigenvalue problem form (Kleiber and Hien 1992)

$$[A] \{q\} = \lambda \{q\}; \quad (34)$$

with

$$\begin{aligned} \lambda &= 1/\lambda^*; \\ [A] &= [V]^{-T} [K_g] [V]^{-1}; \\ \{q\} &= [V] \{q^*\}. \end{aligned} \quad (35)$$



Eq. (34) is the governing equation for buckling analysis of laminated composite plates. Finally, the problem reduces to solving a standard eigenvalue problem. In deterministic environment, solution of this equation yields the critical inplane load. However, in random environment, further analysis is required to obtain the solution.

Since the matrix  $[A]$  is random in nature involving uncertain material properties, the eigen values  $\lambda$  and eigen vectors  $\{q\}$  also become random. Eq. (32) can be solved with the help of perturbation analysis or Monte Carlo simulation to obtain the second order statistics of the buckling load for laminated composite plates with different boundary conditions.

### 3. Solutions- perturbation technique

We consider now a class of problems where the random variation is very small as compared to the mean of the material properties. Properties of most engineering structures, including composites belong to this class. Further, it is quite logical to assume that the dispersion in derived quantities like  $[A]$ ,  $\lambda$  and  $\{q\}$  are also small as compared to their mean values.

A random variable (Nigam 1983) may be broken up as the sum of its mean and zero mean random part as

$$[A] = [\bar{A}] + [A^r]; \quad \lambda = \bar{\lambda} + \lambda^r; \quad \{q\} = \{\bar{q}\} + \{q^r\}; \quad (36)$$

where over bar denotes the mean value and superscript ' $r$ ' denotes the zero mean random part.

Substitution of Eq. (36) in Eq. (34), yields

$$([\bar{A}] + [A^r])(\{\bar{q}_j\} + \{q_j^r\}) = (\bar{\lambda}_j + \lambda_j^r)(\{\bar{q}_j\} + \{q_j^r\}) \quad (37)$$

The perturbed eigenvectors are normalized by using the form (Franklin 1968)

$$\{q_j^r\} = \sum_{k=1}^n (C_{jk}^r) \{\bar{q}_k\} \quad \text{with } (C_{kk}^r = 0). \quad (38)$$

where the  $C_{jk}^r$  for  $j \neq k$  are the small coefficient.

If the components of the matrix  $[A^r]$  are very small, as discussed earlier, Eq. (37) becomes

$$\text{Zeroth order:} \quad [\bar{A}]\{\bar{q}_j\} = \bar{\lambda}_j\{\bar{q}_j\}; \quad (39)$$

$$\text{First order:} \quad [\bar{A}]\{q_j^r\} + [A^r]\{\bar{q}_j\} = \lambda_j^r\{\bar{q}_j\} + \bar{\lambda}_j\{q_j^r\}. \quad (40)$$

To compute the unknowns  $\lambda_j^r$  and  $\{q_j^r\}$  we will use the principle of biorthogonality (Franklin 1968). Let  $\{\bar{q}_1\}, \{\bar{q}_2\}, \dots, \{\bar{q}_n\}$  be the eigen vectors corresponding to the distinct eigen values  $\bar{\lambda}_1, \bar{\lambda}_2, \dots, \bar{\lambda}_n$  of an  $n \times n$  matrix  $[A]$ . Assume  $\bar{\lambda}_i \neq \bar{\lambda}_j$ . Let  $\{\bar{v}_1\}, \{\bar{v}_2\}, \dots, \{\bar{v}_n\}$  be the eigen vectors corresponding to the eigen values  $\bar{\lambda}_1', \bar{\lambda}_2', \dots, \bar{\lambda}_n'$  of  $[\bar{A}^T]$  then

$$(\{\bar{q}_i\}, \{\bar{v}_i\}) \neq 0; \quad (\{\bar{q}_i\}, \{\bar{v}_j\}) = 0 \quad (\text{for } i \neq j); \quad (i, j = 1, 2, \dots, n) \quad (41)$$

To solve Eq. (40), we will use the eigenvectors  $\{\bar{v}_1\}, \{\bar{v}_2\}, \dots, \{\bar{v}_n\}$  of  $[\bar{A}^T]$ . By normalization

at Eq. (38), the perturbation  $\{q_j^r\}$  is a combination of  $\{\bar{q}_k\}$  for  $j \neq k$ . Therefore,  $(\{q_j^r\}, \{\bar{v}_j\}) = 0$ . Now Eq. (40), yields (Franklin 1968)

$$\lambda_j^r = ([A^r])\{\bar{q}_j\}, \{\bar{v}_j\} / (\{\bar{q}_j\}, \{\bar{v}_j\}); \quad (j = 1, \dots, n). \quad (42)$$

For the present case, as discussed earlier,  $[A]$ ,  $\lambda$  and  $\{q\}$  are random because of the material properties. Let  $b_1, b_2, \dots, b_n$  denote the random material properties. Following Eq. (36),  $b_i$  can be expressed as

$$b_i = \bar{b}_i + b_i^r. \quad (43)$$

The stochastic finite element method based on the perturbation technique has been found to be accurate and efficient (e.g., Kareem and Sun 1990, Kleiber and Hien 1992, Vanmarcke and Grigoriu 1983). According to this method, the random variables  $[A]$ ,  $\lambda$  and  $\{q\}$  are expressed by Taylor's series expansion. The expression, with center at the mean value of  $b_i$  and keeping only up to first order terms, is

$$\lambda_j^r = \sum_{i=1}^m \bar{\lambda}_{j,i} b_i^r; \quad \{q_j^r\} = \sum_{i=1}^m \{\bar{q}_{j,i}\} b_i^r; \quad [A^r] = \sum_{i=1}^m [\bar{A}_{,i}] b_i^r; \quad (44)$$

where,  $i$  denotes partial differentiation with respect to  $b_i$ .

Using Eqs. (42) and (44), we have

$$\bar{\lambda}_{j,i} = (\{\bar{A}_{,i}\} \{\bar{q}_j\}, \{\bar{v}_j\}) / (\{\bar{q}_j\}, \{\bar{v}_j\}); \quad (j = 1, \dots, n); \quad (45)$$

The covariance of the eigen value can now be expressed as

$$\text{Cov}(\lambda_j, \lambda_p) = \sum_{i=1}^m \sum_{k=1}^m \bar{\lambda}_{j,i} \bar{\lambda}_{p,k} \text{Cov}(b_i, b_k); \quad (46)$$

where  $\text{Cov}(b_i, b_k)$  is the covariance between  $b_i$  and  $b_k$ .

#### 4. Numerical results and discussion

The method outlined has been used to obtain the second order statistics of the buckling load of laminated composite plates with random material properties. All of the laminae are assumed to be of the same thickness and made up of the same material. Though the approach is valid for different lamina thickness and material properties, the assumption reduces the size of the problem and results in many fold reductions in the calculation efforts. The results have been compared with Monte Carlo simulation and those available in the literature. A nine noded Langaragian isoparametric element, which result in 63 DOFs for the HSDT model, was used for discretizing the laminate. The nine noded Langaragian elements were found to be quite stable and full and reduced integration rules did not have any significant effect on the results for thick plates. Hence, all the results reported in this work have been obtained by employing the full  $(3 \times 3)$  integration rule. Based on

convergence, a  $(4 \times 4)$  mesh has been used throughout for the study. The following non-dimensional buckling load has been used in this study

$$N_{cr} = \bar{N}_{cr} b^2 / (\bar{E}_{22} h^3)$$

The results for laminated composite square plates with three stacking sequences,  $[30^0/-30^0/30^0/-30^0]$ ,  $[45^0/-45^0/45^0/-45^0]$  and  $[60^0/-60^0/60^0/-60^0]$  with CCCC, CFCF and SSSS boundary conditions where, for example, CFCF implies at  $x=0$ , clamped;  $x=a$ , clamped;  $y=0$ , free;  $y=b$ , free, are presented for the ratio of the SD to mean of material properties varying from 0 percent to 20 percent (Liu *et al.* 1986) for  $b/h=5$  and 10 subjected to inplane compressive load along  $y$  direction. The lamina material properties  $E_{11}$ ,  $E_{22}$ ,  $G_{12}$ ,  $\nu_{12}$ ,  $G_{13}$  and  $G_{23}$  are modeled as random variables (Lin and Kam 2000). Here  $E_{11}$  and  $E_{22}$  are longitudinal and transverse elastic moduli, respectively.  $G_{12}$  is in plane shear modulus,  $G_{13}$  and  $G_{23}$  are out of plane shear moduli and  $\nu_{12}$  is the Poisson ratio. These RVs are selected as

$$b_1 = E_{11}, b_2 = E_{22}, b_3 = G_{12}, b_4 = G_{13}, b_5 = G_{23}, \text{ and } b_6 = \nu_{12}.$$

The following dimensionless mean orthotropic material properties have been used in the present investigation (e.g., Noor 1975, Putcha and Reddy 1986, Reddy and Khdeir 1989):  $\bar{E}_{11}=40\bar{E}_{22}$ ,  $\bar{G}_{12}=0.6\bar{E}_{22}$ ,  $\bar{G}_{23}=0.5\bar{E}_{22}$  and  $\bar{\nu}_{12}=0.25$ . It is assumed that  $\bar{G}_{13}=\bar{G}_{12}$  and  $\bar{\nu}_{13}=\bar{\nu}_{12}$  for the above material (Putcha and Reddy 1986).

The boundary conditions for clamped, simply supported and free edges used for the present investigation are given as:

All edges clamped (CCCC):

$$u = v = w = \phi_x = \phi_y = \theta_x = \theta_y = 0, \text{ at } x = 0, a \text{ and } y = 0, b;$$

All edges simply supported (SSSS)

$$v = w = \theta_y = \phi_y = 0, \text{ at } x = 0, a ; u = w = \theta_x = \phi_x = 0, \text{ at } y = 0, b;$$

Alternate edges clamped and free (CFCF):

$$u = v = w = \phi_x = \phi_y = \theta_x = \theta_y = 0, \text{ at } x = 0, a; u \neq v \neq w \neq \phi_x \neq \phi_y \neq \theta_x \neq \theta_y \neq 0, y = 0, b.$$

## 4.1 Validation study

### 4.1.1 Mean buckling load

The accuracy of the proposed finite element model is validated by comparing the results with those available in the literature. The nondimensionalized mean buckling loads for a  $[0^0/90^0]$ ,  $[0^0/90^0/0^0/90^0]$  and  $[0^0/90^0/0^0/90^0/0^0/90^0]$  all edges simply supported antisymmetric cross-ply square plate subjected to axial compressive load has been obtained with length to thickness ratio  $a/h=10$  by using higher order shear deformation theory. The results are presented in Table 1 and compared with those obtained with other methods (e.g., Noor 1975, Putcha and Reddy 1986, Reddy and Khdeir 1989). The results have also been obtained using first order shear deformation theory (FSDT), which are also listed in Table 1. It is seen that the present finite element method yields excellent results. The HSDT gives higher value of buckling load for two layers anti-symmetric laminate while, it gives lower values for other two laminates considered as compared to FSDT.

Table 1 Comparison of nondimensionalised mean buckling loads,  $N_{cr}$  of a simply supported anti symmetric square laminates ( $N_y = N_{xy} = 0$ ,  $a/h = 10$ )

Source	Nondimensionalised mean buckling load		
	$[0^\circ/90^\circ]$	$[0^\circ/90^\circ/0^\circ/90^\circ]$	$[0^\circ/90^\circ/0^\circ/90^\circ/0^\circ/90^\circ]$
Noor [23] <sup>a</sup>	10.817	21.280	23.669
HSDT [24] <sup>b</sup>	11.569	22.582	24.462
HSDT [24] <sup>c</sup>	11.563	22.579	24.460
HSDT [25] <sup>d</sup>	11.563	22.579	24.460
HSDT <sup>e</sup>	11.569	22.618	24.506
FSDT <sup>(e)</sup>	11.352	22.916	24.612

<sup>a</sup>Results obtained by applying a finite difference scheme to the equation of the 3-D elasticity theory. <sup>b</sup>Results obtained using the FEM solution. <sup>c</sup>Results using Navier solution. <sup>d</sup>Results obtained using exact method. <sup>e</sup>Results obtained with  $C^0$  finite element presented in this paper.

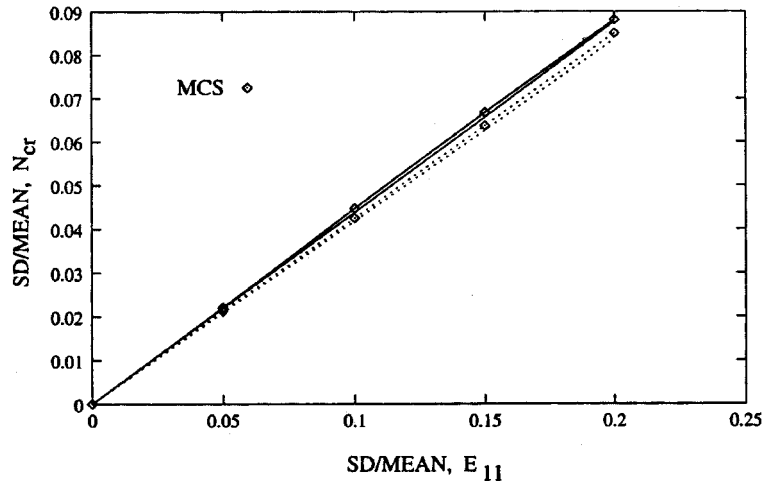


Fig. 2 Validation of results from Monte Carlo simulation with the present approach,  $[0^\circ/90^\circ]$  square laminate, with  $b/h = 5$ . Key: — : HSDT, ..... : FSDT

#### 4.1.2 Standard deviation of buckling load

Fig. 2 shows the validation of the results by the present approach using HSDT and FSDT with Monte Carlo simulation for  $[0^\circ/90^\circ]$  laminated composite square plates with all edges simply supported,  $b/h = 5$ , having taken only one material property  $E_{11}$  random. For MCS approach, the samples are generated using NAG subroutine to fit the desired mean and standard deviation (SD) of the material property. These samples are used in Eq. (34), which is solved repeatedly adopting conventional eigen value solution procedure to generate a sample of the buckling load. This sample is processed to obtain the mean and SD. Both HSDT and FSDT results are in overall good agreement. It can be concluded from the comparison that the first order perturbation technique is quite accurate for the range of SD to mean taken in the study. It can be further concluded that compared to FSDT the HSDT results are more close to respective MCS results, which is considered to be exact method in uncertainty analysis. However, These differences are very small.

Table 2 Nondimensionalized mean buckling loads,  $N_{cr}$  of laminated composite plates with different support conditions ( $N_x = N_{xy} = 0$ ,  $b/a = 1$ )

Support conditions	Nondimensionalised mean buckling load					
	$[60^\circ/-60^\circ/60^\circ/-60^\circ]$		$[30^\circ/-30^\circ/30^\circ/-30^\circ]$		$[45^\circ/-45^\circ/45^\circ/-45^\circ]$	
	$b/h = 5$	$b/h = 10$	$b/h = 5$	$b/h = 10$	$b/h = 5$	$b/h = 10$
CCCC	13.2984	40.7803	9.9566	25.4798	12.0520	35.4335
CFCF	8.3345	17.1185	5.8923	12.0925	7.5939	16.4740
SSSS	12.9733	33.0347	9.2449	22.5867	11.6835	30.9250

## 4.2 Mean buckling load

Table 2 presents nondimensionalized mean buckling loads with  $b/h = 5$  and 10 for stacking sequences of  $[30^\circ/-30^\circ/30^\circ/-30^\circ]$ ,  $[45^\circ/-45^\circ/45^\circ/-45^\circ]$  and  $[60^\circ/-60^\circ/60^\circ/-60^\circ]$  graphite-epoxy square plates with CCCC, CFCF and SSSS boundary conditions using HSDT subjected to transverse compressive load. For both  $b/h$  ratios, it is observed that the nondimensionalized-buckling load increases as the lamination angle increases. The mean buckling load is more in case of the plate with all edges clamped for a fixed  $b/h$  ratio and lamination angle, while the plate CFCF boundary condition buckle at less load as compared to the rest of the boundary conditions investigated. There is significant change in non-dimensionalised buckling load as the  $b/h$  ratio changes for all combinations of edge conditions considered.

## 4.3 Standard deviation of buckling load

The SD/mean of the buckling load have a linear variation with the change in the material properties. The rate of scatter depends on the thickness ratio, edge condition and the material property being considered. The behavior also shows sensitivity to the lay up angle.

### 4.3.1 Simultaneous variation in material properties

From application point of view, it is appropriate to consider the case where all the properties vary simultaneously. Figs. 3(a) and (b) present the normalized SD of the nondimensionalized buckling load with SD of all the material properties varying simultaneously each assuming the same value for the ratio of its SD to mean for  $[60^\circ/-60^\circ/60^\circ/-60^\circ]$  square laminate with  $b/h = 5$  and 10, respectively. Figs. 3(c) and (d) represent corresponding behaviour for  $[30^\circ/-30^\circ/30^\circ/-30^\circ]$  and Figs. 3(e) and (f) for  $[45^\circ/-45^\circ/45^\circ/-45^\circ]$  square laminates.

For lamination angle  $60^\circ$ , it is observed that the plate with CCCC boundary condition is more sensitive while, CFCF plate is less sensitive for  $b/h = 5$ . For  $b/h = 10$ , it is interesting to note that SSSS plate is more sensitive and CFCF plate is less sensitive. It is also observed that the effect of input RVs on scatter in nondimensionalized buckling load is most dominant for CCCC plate with  $b/h = 5$ , while its effect is least dominant on CFCF plate with same thickness ratio.

For lamination angle  $30^\circ$ , the CCCC plate is more sensitive for  $b/h = 5$ , while, it is less sensitive for CFCF plate. It is seen that for  $b/h = 10$ , the SSSS plate is more sensitive and CCCC plate is less sensitive as compared to other boundary conditions.

For lamination angle  $45^\circ$ , the CCCC and SSSS plates show sensitivity of the same order of magnitude but more as compared to CFCF plate for  $b/h = 5$ , while, all three types of plates show

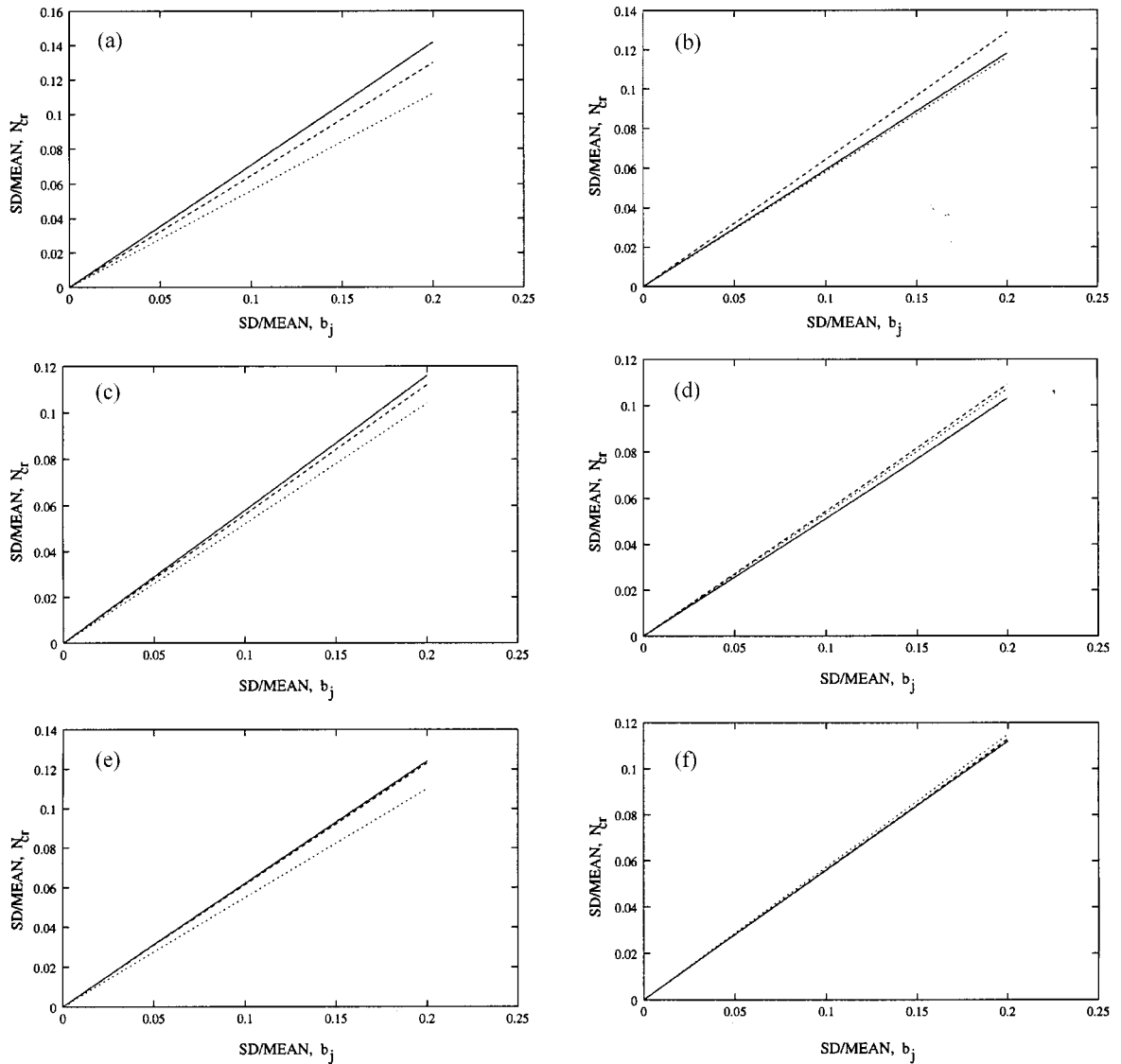


Fig. 3 Variation of SD/mean of the nondimensionalized buckling loads with SD of basic material properties, square laminate with all basic material properties changing simultaneously: (a)  $b/h = 5$ ;  $[60^\circ/-60^\circ/60^\circ/-60^\circ]$ ; (b)  $b/h = 10$  and  $[60^\circ/-60^\circ/60^\circ/-60^\circ]$ ; (c)  $b/h = 5$  and  $[30^\circ/-30^\circ/30^\circ/-30^\circ]$ ; (d)  $b/h = 10$  and  $[30^\circ/-30^\circ/30^\circ/-30^\circ]$ ; (e)  $b/h = 5$  and  $[45^\circ/-45^\circ/45^\circ/-45^\circ]$  (f)  $b/h = 10$  and  $[45^\circ/-45^\circ/45^\circ/-45^\circ]$ .

Key: — : CCCC, ..... : CFCF, ---- : SSSS

almost same order of sensitivity for  $b/h = 10$ .

#### 4.3.2 Individual variation of material properties

$[60^\circ/-60^\circ/60^\circ/-60^\circ]$  Ant-symmetric square laminate:

Figs. 4(a)–(f) and 5(a)–(f) present the variation of SD/mean of the nondimensionalized buckling loads for a  $[60^\circ/-60^\circ/60^\circ/-60^\circ]$  laminate with changes in only one material property at a time,

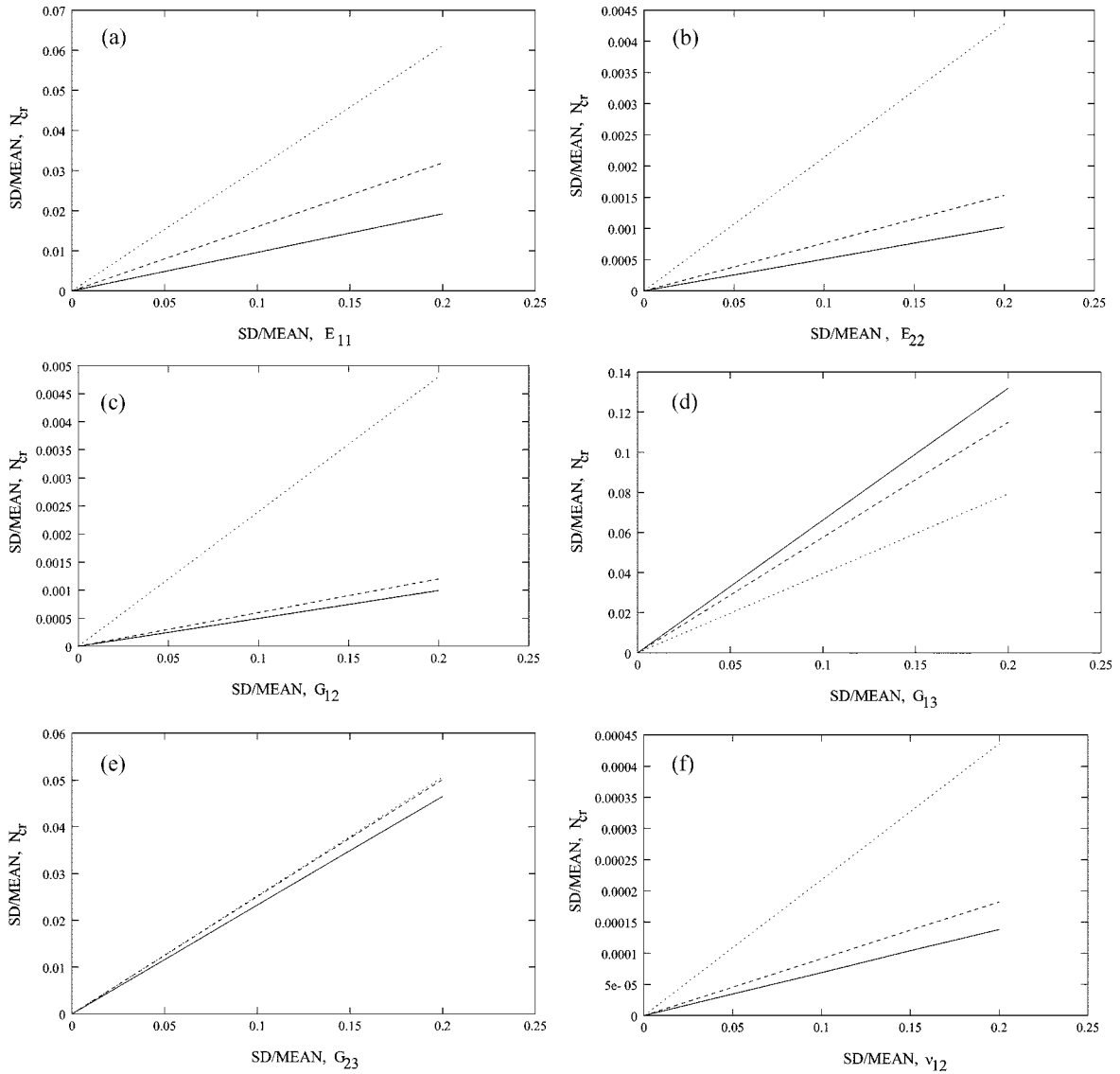


Fig. 4 Variation of SD/mean of the nondimensionalized buckling loads with SD of basic material properties,  $[60^\circ/-60^\circ/60^\circ/-60^\circ]$  square laminate, with  $b/h = 5$ : (a) Only  $E_{11}$  varying; (b) only  $E_{22}$  varying; (c) only  $G_{12}$  varying; (d) only  $G_{13}$  varying; (e) only  $G_{23}$  varying; (f) only  $\nu_{12}$  varying. Key: As in Fig. 3

keeping others as deterministic for  $b/h = 5$  and 10, respectively.

For  $b/h = 5$ , the effect of individual variation of  $E_{11}$ ,  $E_{22}$ ,  $G_{12}$  and  $\nu_{12}$  on scatter in the buckling load is strongest for plate with CFCF while it is lowest for CCCC. The effect of  $G_{13}$  is largest for CCCC plate and lowest for CFCF plate. The influence of  $G_{23}$  is largest for CFCF but of same order of magnitude for SSSS plate while, CCCC plate is least affected. In general, the scattering in buckling load is most affected with changes in  $G_{13}$  and least affected with  $\nu_{12}$  for all support conditions considered. In overall behavior, the CCCC plate exhibits the maximum scatter with  $G_{13}$  changing as compared to any other support conditions.

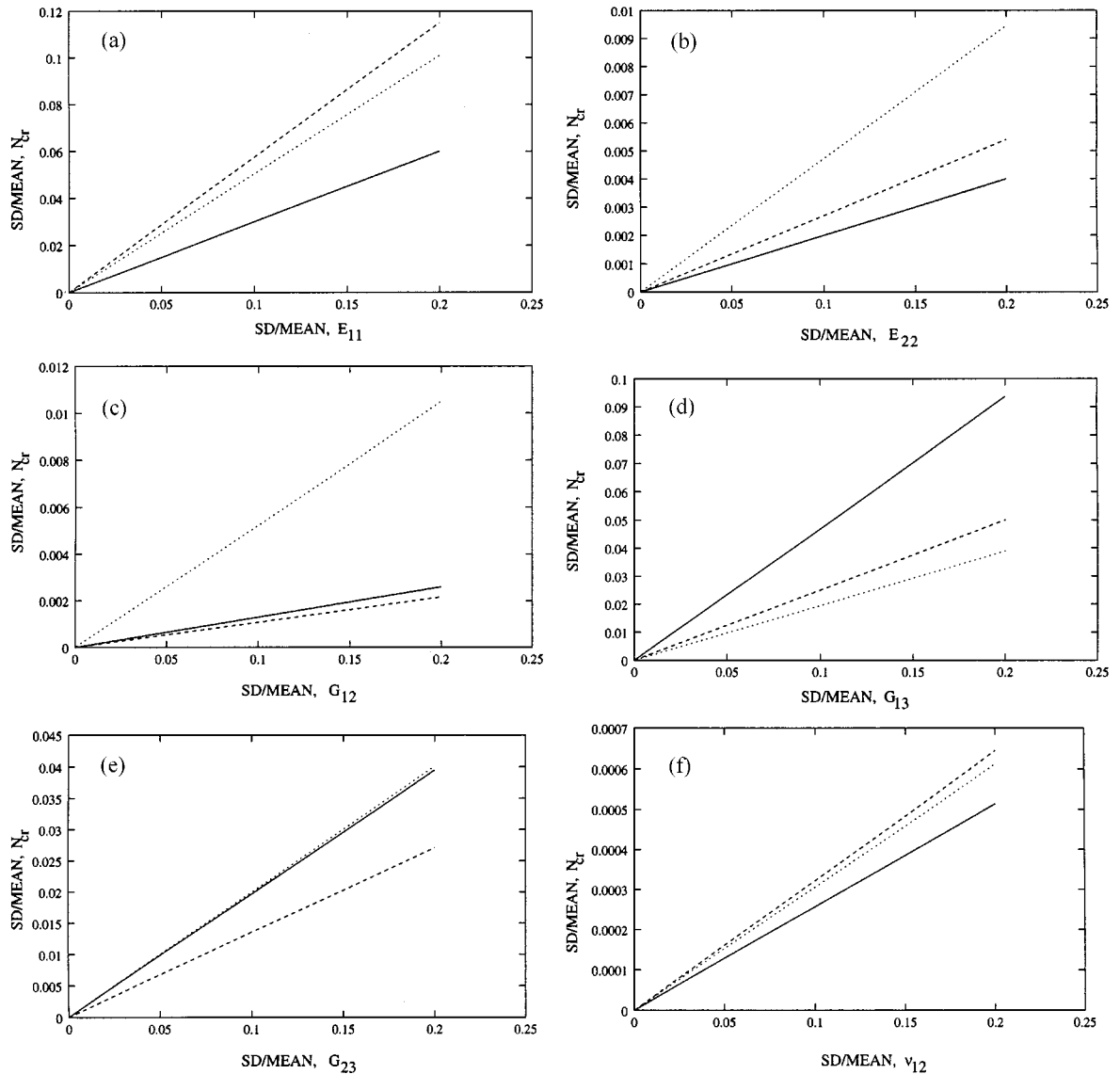


Fig. 5 Variation of SD/mean of the nondimensionalized buckling loads with SD of basic material properties,  $[60^0/-60^0/60^0/-60^0]$  square laminate, with  $b/h = 10$ : (a) Only  $E_{11}$  varying; (b) only  $E_{22}$  varying; (c) only  $G_{12}$  varying; (d) only  $G_{13}$  varying; (e) only  $G_{23}$  varying; (f) only  $v_{12}$  varying. Key: As in Fig. 3

For  $b/h = 10$ , SSSS plates are most affected with individual changes in  $E_{11}$  and  $v_{12}$ , while CCCC plate is least affected. The effect of  $E_{22}$  is strongest for CFCF and lowest for CCCC plate. The extreme effects of  $G_{12}$  and  $G_{13}$  are largest for CFCF and CCCC respectively and lowest for SSSS and CFCF respectively. The CCCC and CFCF plates are more sensitive to changes in  $G_{23}$  compared to SSSS plate. In over all sense, the SSSS and CFCF plates are most affected with  $E_{11}$ , CCCC plate is most affected with changes in  $G_{13}$  and all types of plates are least affected with changes in  $v_{12}$ .



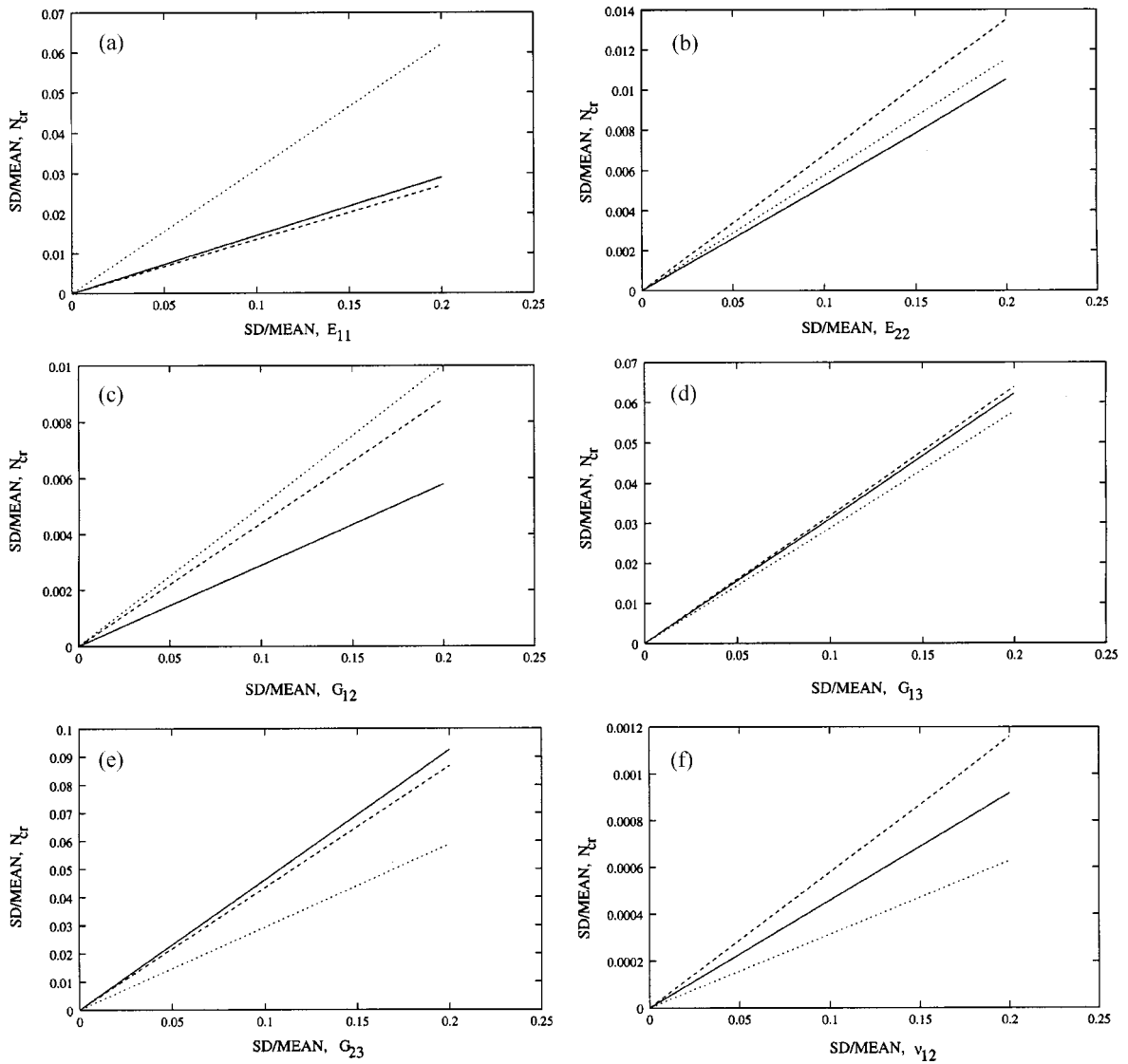


Fig. 6 Variation of SD/mean of the nondimensionalized buckling loads with SD of basic material properties,  $[30^\circ/-30^\circ/30^\circ/-30^\circ]$  square laminate, with  $b/h = 5$ : (a) Only  $E_{11}$  varying; (b) only  $E_{22}$  varying; (c) only  $G_{12}$  varying; (d) only  $G_{13}$  varying; (e) only  $G_{23}$  varying; (f) only  $\nu_{12}$  varying. Key: As in Fig. 3

$[30^\circ/-30^\circ/30^\circ/-30^\circ]$  Anti-symmetric square laminate:

Figs. 6(a)–(f) and 7(a)–(f) show the variation of nondimensionalized buckling loads of  $[30^\circ/-30^\circ/30^\circ/-30^\circ]$  laminate with only one material property random at a time for  $b/h = 5$  and 10, respectively.

For  $b/h = 5$ , the effect of  $G_{13}$  and  $G_{23}$  on dispersion of buckling load is more for plate with SSSS and CCCC, respectively, while dispersion is less for CFCF plate. The influence of  $E_{22}$  and  $\nu_{12}$  for SSSS plate is strongest and lowest for CCCC and CFCF, respectively. The impact of  $E_{11}$  and  $G_{12}$  on dispersion of buckling load is strongest for CFCF plate, while lowest for SSSS and CCCC plates, respectively. The dispersion in CFCF plate buckling is most affected with changes in  $E_{11}$ , while

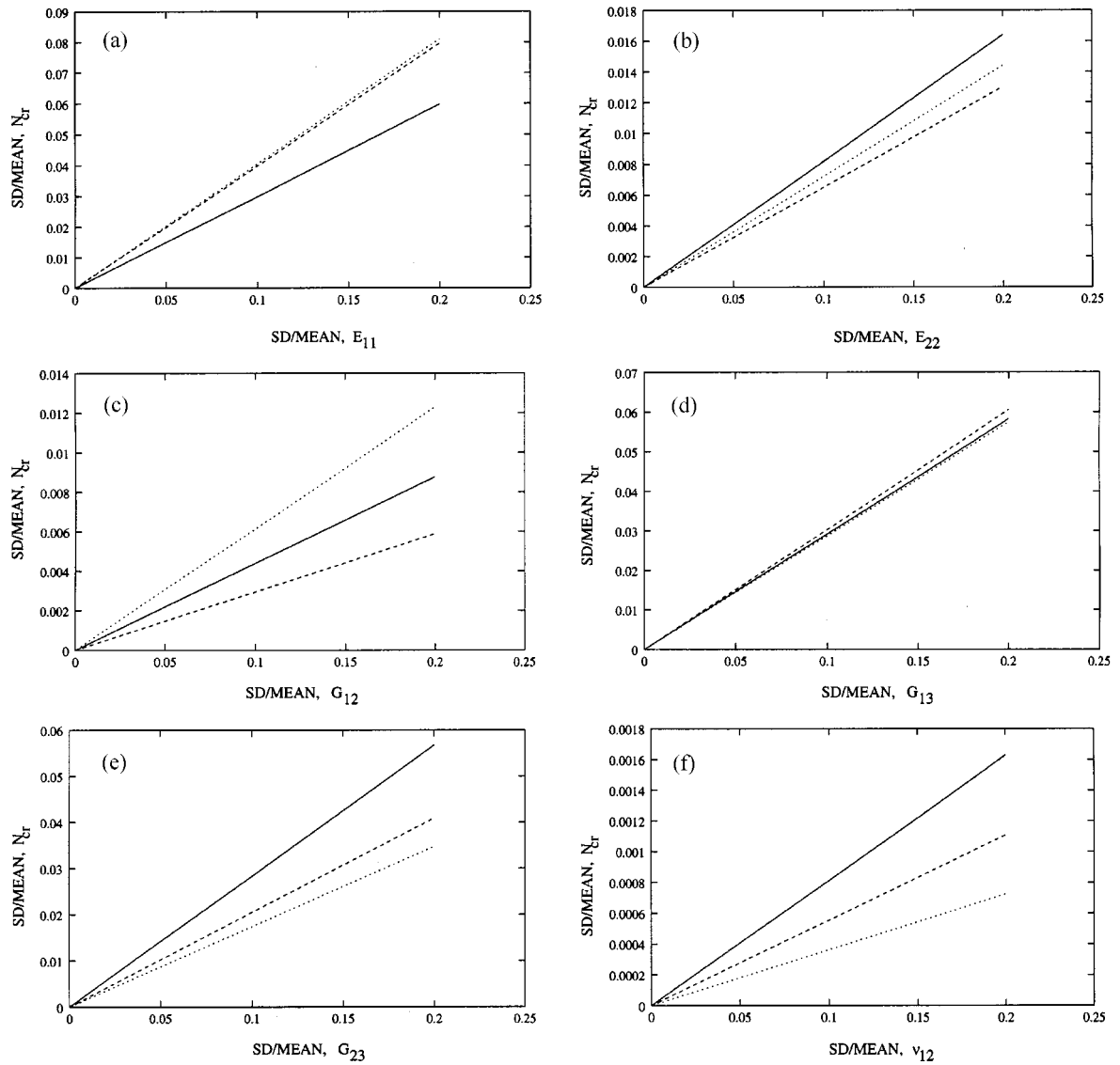


Fig. 7 Variation of SD/mean of the nondimensionalized buckling loads with SD of basic material properties,  $[30^\circ/-30^\circ/30^\circ/-30^\circ]$  square laminate, with  $b/h = 10$ : (a) Only  $E_{11}$  varying; (b) only  $E_{22}$  varying; (c) only  $G_{12}$  varying; (d) only  $G_{13}$  varying; (e) only  $G_{23}$  varying; (f) only  $\nu_{12}$  varying. Key: As in Fig. 3

CCCC and SSSS plates are most affected with  $G_{23}$ . The plates with different boundary conditions are least affected with changes in  $\nu_{12}$ .

For  $b/h = 10$ , with individual variation of  $E_{11}$ ,  $E_{22}$ ,  $G_{12}$  and  $\nu_{12}$ , the CFCF plate is more sensitive, while CCCC plate is less sensitive. The CCCC plate is more sensitive to changes in  $G_{13}$  and  $G_{23}$ , while, CFCF plate has lowest sensitivity for these. In general, plates are most affected with changes in  $G_{13}$  and least affected with  $\nu_{12}$ .

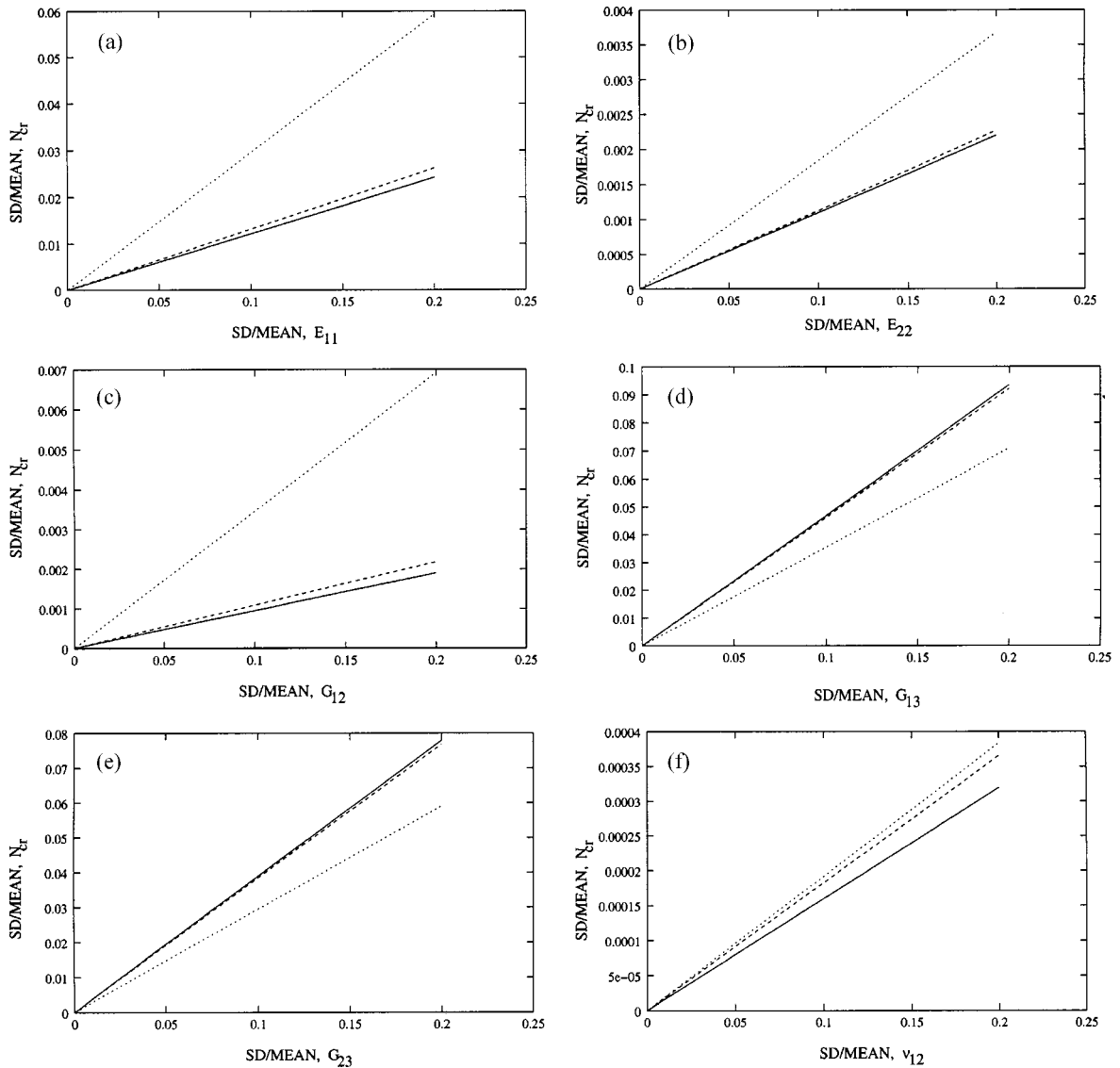


Fig. 8 Variation of SD/mean of the nondimensionalized buckling loads with SD of basic material properties,  $[45^\circ/-45^\circ/45^\circ/-45^\circ]$  square laminate, with  $b/h = 5$ : (a) Only  $E_{11}$  varying; (b) only  $E_{22}$  varying; (c) only  $G_{12}$  varying; (d) only  $G_{13}$  varying; (e) only  $G_{23}$  varying; (f) only  $\nu_{12}$  varying. Key: As in Fig. 3

$[45^\circ/-45^\circ/45^\circ/-45^\circ]$  Anti-symmetric square laminate:

Figs. 8(a)–(f) and 9(a)–(f) present the sensitivity of nondimensionalized buckling loads of  $[45^\circ/-45^\circ/45^\circ/-45^\circ]$  laminate with random changes in only one material property at a time for  $b/h = 5$  and 10, respectively.

For  $b/h = 5$ , the changes in  $E_{11}$ ,  $E_{22}$ ,  $G_{12}$  and  $\nu_{12}$  have largest impact on CFCF plate buckling load scattering and least impact on CCCC plate. The effect of  $G_{13}$  and  $G_{23}$  is strongest for all edges clamped plates, while lowest for CFCF plates. In general, the plate with different boundary

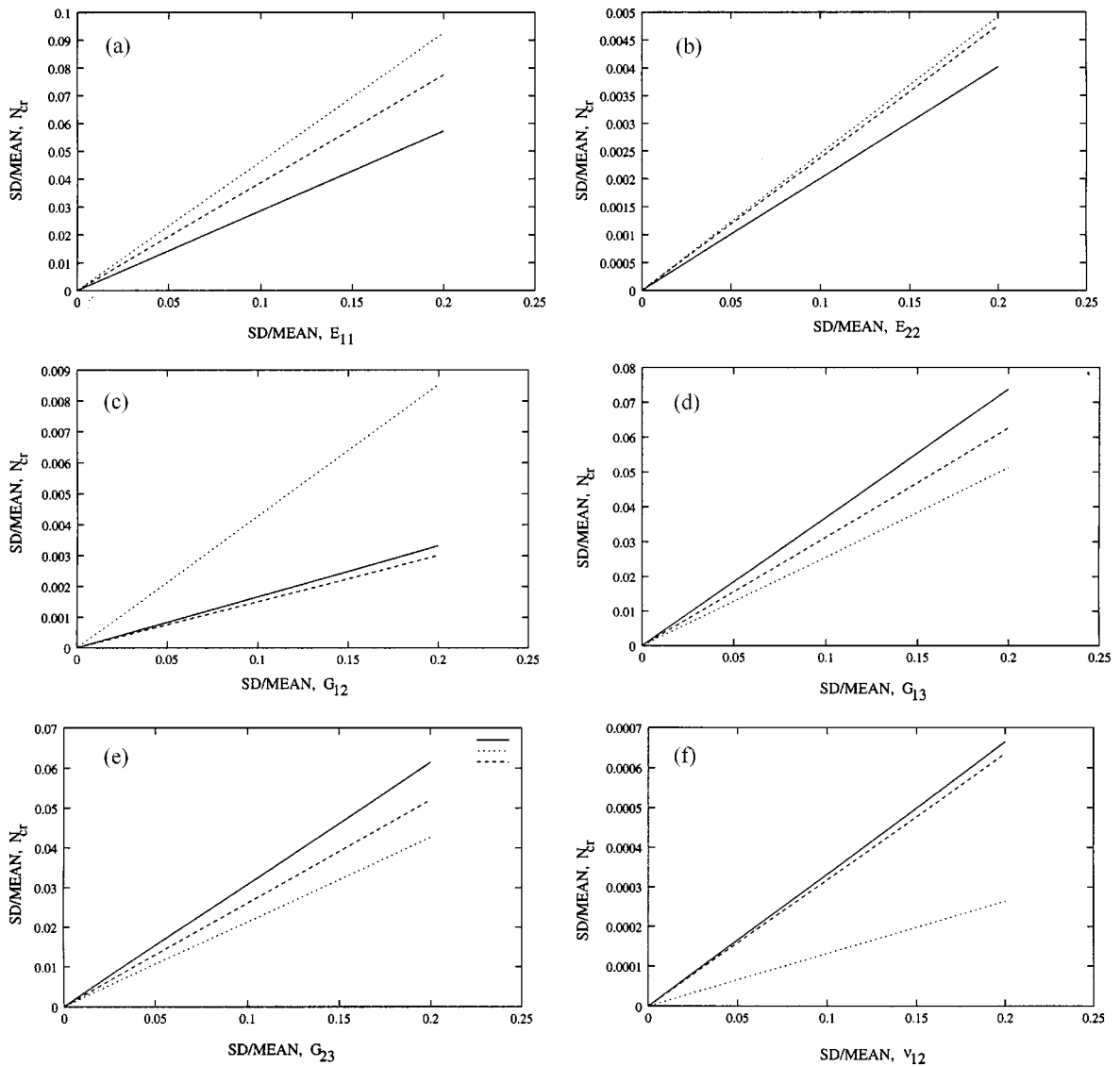


Fig. 9 Variation of SD/mean of the nondimensionalized buckling loads with SD of basic material properties,  $[45^0/-45^0/45^0/-45^0]$  square laminate, with  $b/h = 10$ : (a) Only  $E_{11}$  varying; (b) only  $E_{22}$  varying; (c) only  $G_{12}$  varying; (d) only  $G_{13}$  varying; (e) only  $G_{23}$  varying; (f) only  $\nu_{12}$  varying. Key: As in Fig. 3

conditions are most affected with changes in  $G_{13}$  and it is least affected with  $\nu_{12}$ .

For  $b/h = 10$ , with changes in  $E_{11}$ ,  $E_{22}$  and  $G_{12}$  the CFCF plate has largest sensitivity while lowest sensitivity is shown by CCCC plate for changes in  $E_{11}$  and  $E_{22}$  and SSSS plate for  $G_{12}$ . The effect of  $G_{13}$ ,  $G_{23}$  and  $\nu_{12}$  is strongest for CCCC plates, while it is lowest for CFCF plates. In general the CFCF and SSSS plates are most affected with  $E_{11}$ . The CCCC plate is most affected with SD of  $G_{13}$ . The least dispersion in buckling load is seen with change in SD of  $\nu_{12}$  for all plate types considered.

## 5. Conclusions

A probabilistic study of the buckling behavior of laminated composite plates with different boundary conditions has been carried out using finite element method in conjunction with first order perturbation technique. Though the method uses the assumption of small deviations about the mean values of the random parameters, it has been found to be valid for nonsmall deviations. This may be due to linear relationship between the response and the basic input variables. The following main conclusions can be drawn from the results obtained:

- (1) The dispersion in nondimensionalized buckling load decreases as  $b/h$  ratio changes from 5 to 10 against simultaneous changes in material properties for CCCC plate, while it slightly increases for SSSS plate.
- (2) For a fixed  $b/h$  ratio, the scatter in nondimensionalized buckling load increases as lamination angle increases.
- (3) The CCCC plate with lamination angle  $60^\circ$  and  $b/h = 5$  is most affected, while the CCCC plate with lamination angle  $30^\circ$  and  $b/h = 10$  is least affected with SD of one material property changing at a time.
- (4) For fixed lamination angle, the effect of individual variation of  $E_{11}$ ,  $E_{22}$  and  $G_{12}$  on scatter in buckling load increases as  $b/h$  ratio increase, while the effect of  $G_{13}$  and  $G_{23}$  decreases. The behavior due to changes in  $\nu_{12}$  does not show a pattern.
- (5) The sensitivity of buckling load dispersion to variations in individual material properties is different for different edge support conditions. For lamination angle  $60^\circ$ , the CCCC plate with  $b/h = 5$  is most sensitive to  $G_{13}$ , the SSSS plate with  $b/h = 5$  and 10 is equally most sensitive to  $G_{13}$  and  $E_{11}$ , respectively and the CFCF plate with  $b/h = 10$  is most sensitive to  $E_{11}$ .
- (6) Among all, the sensitivity of CCCC plate with  $b/h = 5$  and lamination angle  $60^\circ$  is highest.
- (7) The effect of  $\nu_{12}$  is least dominant on scatter in nondimensionalised buckling load.

## References

- Cha, P.D., and Gu, W. (1999), "Comparing the perturbed eigensolutions of a generalized and a standard eigen value problem", *J. Sound & Vibration*, **227**(5), 1122-32.
- Englested, S.P., and Reddy, J.N. (1994), "Probabilistic methods for the analysis of metal matrix composite", *Composite Science & Technology*, **50**, 91-107.
- Franklin, J.N. (1968), *Matrix Theory*, Prentice-Hall, Englewood Cliff, N. J.
- Ghosh, A.K., and Dey, S.S. (1994), "Buckling of laminated plates-a simple finite element element based on higher order theory", *Finite Element Analysis and Design*, **15**, 289-302.
- Hinton, E., and Owen, D.R.J. (1984), *Finite Element Software for Plates and Shells*, Pnneridge Press, Swansea.
- Ibrahim, R.A. (1987), "Structural dynamics with parameter uncertainties", *Appl. Mech. Rev.*, **40**, 309-28.
- Kareem, A., and Sun, W.J. (1990), "Dynamic response of structures with uncertain damping", *Eng. Struct.*, **12**, 1-8.
- Kleiber, M., and Hien, T.D. (1992), *The Stochastic Finite Element Method*, John Wiley & Sons.
- Leissa, A.W., and Martin, A.F. (1990), "Vibration and buckling of rectangular of composite plates with variable fiber spacing", *Comp. Struct.*, **14**, 339-57.
- Lin, S.C., and Kam, T.Y. (2000), "Probability failure analysis of transversely loaded composite plates using higher-order second moment method", *J. Eng. Mech.*, ASCE, **126**(8), 812-20.
- Liu, W.K., Belytschko, T., and Mani, A. (1986), "Random field finite elements", *Int. J. Numer. Meth. in Eng.*, **23**, 1831-45.

- Manohar, C.S., and Ibrahim, R.A. (1999), "Progress in structural dynamics with stochastic parameter variations: 1987-1998", *Applied Mechanics Review*, **52**, 177-96.
- Mindlin, R.D. (1951), "Influence of rotary inertia and shear deformation on flexure motions of isotropic elastic plates", *J. Appl. Mech., Transac., ASME*, **18**, 31-38.
- Moita, J.S., Mota Soares, C.M., and Mota Soares, C.A. (1996), "Buckling behavior of laminated composite structures using a discrete higher-order displacement model", *Compos. Struct.*, **35**, 75-92.
- Nakagiri, S., Tatabatake, H., and Tani, S. (1990), "Uncertain eigen value analysis of composite laminated plates by sfem", *Compo. Struct.*, **14**, 9-12.
- Nigam, N. C. (1983), *Introduction to Random Vibrations*, MIT Press, Cambridge, MA.
- Noor, A.K. (1975), "Stability of multi-layered composite plates", *Fibre Science & Technology*, **8**(2), 81-89.
- Putcha, N.S., and Reddy, J.N. (1986), "Stability and natural vibration analysis of laminated plates by using a mixed element based on a refined plate theory", *J. Sound & Vibration*, **104**(8), 285-300.
- Reddy, J.N. (1984), "A simple higher order shear theory for laminated composite plates", *J. Appl. Mech., Transac. of the ASME*, **51**, 745-752.
- Reddy, J.N., and Khdeir, A.A. (1989), "Buckling and vibration of laminated composite plates using various plate theories", *AIAA J.*, **27**(12), 1808-17.
- Reissner, E. (1945), "The effects of transverse shear deformation on the bending of elastic plates", *J. Appl. Mech., Trans, ASME*, **12**, 69-77.
- Salim, S., Iyengar, N.G.R., and Yadav, D. (1998), "Buckling of laminated plates with random material characteristics", *Appl. Compos. Mat.*, **5**, 1-9.
- Shankara, C.A., and Iyengar, N.G.R. (1996), "A  $C^0$  element for the free vibration analysis of laminated composite plates", *J. Sound & Vibration*, **191**(5), 721-38.
- Singh, B.N., Yadav, D., and Iyengar, N.G.R. (2001), "Initial buckling of composite cylindrical panels with random material properties", *Compos. Struct.*, **53**(1), 55-64.
- Vanmarcke, E.H., and Grigoriu, M. (1983), "Stochastic finite element analysis of simple beam", *J. Eng. Mech., ASCE*, **109**, 1203-14.
- Vinckenroy, G.V., and Wilde, W.P. de. (1995), "The use of Monte Carlo techniques in sfem for determination of the structural behavior of composites", *Compos. Struct.*, **32**, 247-53.
- Yadav, D., and Verma, N. (1997), "Buckling of composite circular cylindrical shells with random material properties", *Compos. Struct.*, **37**, 385-91.